

A theoretical and experimental study of the lithiation of ${}^0\text{Cu}_6\text{Sn}_5$ in a lithium-ion battery.

S. Sham ^{a1}, L. Fransson ³, E. Sjöstedt ¹, L. Nordström ¹, B. Johansson ^{1;2} and K. Edström ³

¹Condensed Matter Theory Group, Department of Physics,
Uppsala University, BOX 530, SE-751 21 Uppsala, Sweden

²Applied Materials Physics,
Department of Materials Science and Engineering,
Royal Institute of Technology,
SE-100 44 Stockholm, Sweden

³Department of Materials Chemistry,
Uppsala University, BOX 538, SE-751 21 Uppsala, Sweden

In this work, the mechanism of Li insertion in ${}^0\text{Cu}_6\text{Sn}_5$ to form Li_2CuSn is discussed in detail, based on both theoretical calculations and experimental results. The mechanism is investigated by means of first principles calculations, with the full potential linearized augmented plane wave method, in combination with in situ X-ray diffraction experiments. The ${}^0\text{Cu}_6\text{Sn}_5$ structure, as well as its lithiated products, have been optimized and the electronic charge density calculated in order to study the change in bond character on lithiation. The average insertion voltage of the ${}^0\text{Cu}_6\text{Sn}_5\text{-Li}_2\text{CuSn}$ transformation has been calculated to be 0.378V in good agreement with the experimental value.

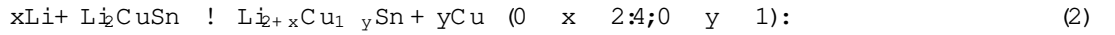
INTRODUCTION

Light weight and compact, lithium-ion batteries [1] are ideal energy storage devices for the use in appliances like laptops, mobile phones and electric vehicles. But there are concerns about the safety of the lithium-ion batteries in their present form because, the most common material used as anodes in these batteries is graphite and its lithiated potential is very close to that of the lithium. The study of intermetallic insertion electrodes, as possible replacements for graphite, has recently attracted a lot of attention. Examples of such structures are InSb [2, 3] and Cu₂Sb [4]. The desirable characteristics for an ideal anode material include the capability of reversible Li intercalation/insertion while maintaining the stability of the structure. One of the materials that possess these qualities and has been found to be a possible alternative for graphite in lithium-ion batteries is ⁰Cu₆Sn₅ [5, 6, 7, 8].

In situ X-ray diffraction (XRD) studies have shown that, during the electrochemical reaction of ⁰Cu₆Sn₅ with lithium, a Li₂CuSn-type structure is formed [6, 7, 8]. The ideal reaction for this phase transformation can be described by:



Further lithiation of the Li₂CuSn structure results in further extrusion of Cu from the structure, to finally form Li_{4.4}Sn (the maximum lithiated Sn-phase). This reaction is described as:



These reactions were recently supported by the in situ ¹¹⁹Sn-Mössbauer spectroscopy measurements [8]. When the lithiation process is interrupted, to only involve reaction (1) (above 0.2V vs. Li/Li⁺), the material shows a reversible and stable lithium insertion behaviour with a capacity of 200mAh/g. If the material is fully lithiated to form Li_{4.4}Sn, the cycling stability is dramatically affected and the ability to insert lithium reversibly gradually declines. The reason for this is believed to originate from the large structural rearrangements that occurs in reaction (2), along with the extrusion of Cu. The experimental data provides information on the main processes that occurs on lithiation of the ⁰Cu₆Sn₅ structure. The detailed mechanisms of reactions (1) and (2) are, however, unclear. For example the positions of the initial Li in the ⁰Cu₆Sn₅ structure and the starting point of Cu extrusion from the structure are not known. Although there have been suggestions regarding the mechanism of the phase change from ⁰Cu₆Sn₅ to Li₂CuSn [5, 6], there exists no experimental measurement or theoretical calculation to back these suggestions. In the present work we have performed ab-initio calculations to investigate this mechanism. The ⁰Cu₆Sn₅ structure has been optimized and the calculations performed to determine the average insertion voltage for the Cu₆Sn₅-Li₂CuSn transformation.

The paper is arranged in the following manner. Section II gives the details of the calculations and experiments. The results of the structural optimization and electric field gradients are presented in section III A. Section III B deals with the discussions about the charge densities and the nature of the bonds in ⁰Cu₆Sn₅ and Li₂CuSn compounds. In section III C the results and some ideas about the mechanism of lithiation of ⁰Cu₆Sn₅ are presented. Finally section IV comprises of the conclusions of our work.

METHODOLOGY

Theoretical

The total energy calculations are performed using the full potential linear augmented plane wave (FP-LAPW) method using the WIEN97 code [9]. The high-lying Cu and Sn semi-core d states are treated using local orbitals. The calculations are performed within the local density approximation (LDA). The scalar relativistic equations are used in a self-consistent scheme. These calculations are performed using 115 and 204 k points in the irreducible Brillouin zone (IBZ) for ⁰Cu₆Sn₅ and Li₂CuSn respectively. The structural optimization for ⁰Cu₆Sn₅ is performed using 4 k points in the IBZ.

⁰Cu₆Sn₅ has a monoclinic lattice with the space group C2/c (no.15). The calculations are performed at the experimental lattice parameters [10] (a= 11.022Å, b= 7.282Å, c= 9.827Å). However, we have used the theoretically optimized atom positions given in table I for all the calculations. The conventional unit cell for ⁰Cu₆Sn₅ is presented in figure 1. Structurally Li₂CuSn exists in a cubic phase with the space group F43m (no.216) [11]. The calculations are performed at the experimental lattice parameter of a= 6.282Å and the atomic positions are given in table I.

Experimental

$^{63}\text{Cu}_6\text{Sn}_5$ was synthesised by a high-energy ball-milling procedure, as described elsewhere [6]. Electrodes were made by mixing 90 wt% Cu_6Sn_5 powder with 5 wt% carbon black and 5 wt% EPDM rubber binder. The slurry was spread onto a Ni-foil. Two-electrode "coo-ee-bag" $\text{Cu}_6\text{Sn}_5/\text{Li}$ -cells were made as described earlier [8]. Cell cycling was performed on a Digatron BTS-600 battery tester, in galvanostatic mode, with a current density of $0.022 \text{ mA}/\text{cm}^2$.

In situ X-ray diffraction data of Cu_6Sn_5 electrodes in $\text{Li}/\text{Cu}_6\text{Sn}_5$ cells were collected during the initial discharge in transmission mode using a STOE and CIE GmbH STADI powder diffractometer fitted with a position-sensitive detector ($\text{CuK}_{\alpha 1}$ radiation). Measurements were recorded with a fixed detector covering $38.8^\circ - 45.3^\circ$ in 2θ while a constant current of 0.15 mA was applied by a MacPile II instrument.

Table I: The optimized and the experimental [10] atomic positions in the $^{63}\text{Cu}_6\text{Sn}_5$ unit cell and the experimental atomic positions in the Li_2CuSn unit cell [11]. The atomic designations are as in Ref. 10 and the site designations are in Wyckoff notations [12].

Compound	Atom	site	optimized positions x, y, z	experimental positions x, y, z
$^{63}\text{Cu}_6\text{Sn}_5$	Cu1	8f	0.10200, 0.47500, 0.20610	0.10096, 0.47297, 0.20236
	Cu2	8f	0.30570, 0.50600, 0.60650	0.30620, 0.50404, 0.60972
	Cu3	4a	0, 0, 0	0, 0, 0
	CuA	4e	0, 0.16800, $\frac{1}{4}$	0, 0.16020, $\frac{1}{4}$
	Sn1	8f	0.39000, 0.16500, 0.53000	0.39106, 0.16250, 0.52867
	Sn2	8f	0.28000, 0.65000, 0.35650	0.28518, 0.65499, 0.35792
	Sn3	4e	0, 0.80500, $\frac{1}{4}$	0, 0.79892, $\frac{1}{4}$
Li_2CuSn	Cu	4c		$\frac{1}{4}, \frac{1}{4}, \frac{1}{4}$
	Sn	4a		0, 0, 0
	Li	24f		$\frac{1}{2}, 0, 0$
	Li	4c		$\frac{3}{4}, \frac{1}{4}, \frac{1}{4}$

RESULTS AND DISCUSSION

The structural optimization and the electric field gradients

First, we shall discuss the importance of the atomic relaxations in $^{63}\text{Cu}_6\text{Sn}_5$. The base centered monoclinic structure of $^{63}\text{Cu}_6\text{Sn}_5$ [10] has four different kinds of Cu atoms at sites 4e, 4a and 8f and three different kinds of Sn atoms at site 4e and 8f with a total of 4 formula-units (44 atoms) per conventional unit cell (from now on referred to as the CUC). The calculations performed for the experimental atomic positions [10] show that there are forces on the atoms which can not be neglected, so the relaxation of the structure is needed. On complete relaxation of the atomic positions, there is a gain in energy of $2.19 \text{ mRy}/\text{formula-unit}$ of Cu_6Sn_5 . The optimized atomic positions are presented in table I.

The experimentally observed parameter that is sensitive to small structural changes and depends on the electronic charge distribution in a crystal is the electric field gradient (EFG). We have determined the EFG and the asymmetry parameter for both the relaxed and unrelaxed structures for comparison with future experimental work and the values are presented in table II. The details of the method of calculation of the EFG and the asymmetry parameter using FP-LAPW are given elsewhere [13, 14]. On relaxation of the structure the magnitude of V_{zz} for Sn1 and Sn2 increases and decreases for Sn3. The asymmetry parameter shows an increase for Sn1 and Sn3 and decrease for Sn2. For all the four kinds of Cu atoms the magnitude of V_{zz} increases and the asymmetry parameter decreases on the structural relaxation of $^{63}\text{Cu}_6\text{Sn}_5$.

In the case of Li_2CuSn there are no forces on the atoms and so the atomic relaxations are not needed and all the further calculations are performed with the atoms at the ideal positions. Since the atoms in Li_2CuSn are present at high symmetry positions of a cubic lattice the theoretical EFG vanishes.

Table II: The electric field gradient (V_{zz}) and the asymmetry parameter (η) for different Cu and Sn sites in the $^{63}\text{Cu}_6\text{Sn}_5$ unit cell with the optimized and the experimental [10] atomic positions.

Atom	Optim ized structure V_{zz} ($\times 10^{21}$ V /m ²)		Experim ental structure [10] V_{zz} ($\times 10^{21}$ V /m ²)	
Cu1	-4.05	0.326	-3.84	0.385
Cu2	-4.46	0.153	-4.32	0.163
Cu3	-4.58	0.257	-4.40	0.331
CuA	1.42	0.508	1.36	0.707
Sn1	-10.35	0.743	-10.10	0.644
Sn2	4.18	0.519	3.80	0.806
Sn3	-14.11	0.718	-15.02	0.696

The electron charge density

Figure ?? and ?? show the difference between the crystalline charge and the superposed atomic charge for $^0\text{-Cu}_6\text{Sn}_5$ in (102) plane and for Li_2CuSn in (110) plane respectively. It is clear from figure 2 that in case of $^0\text{-Cu}_6\text{Sn}_5$ the Sn atoms gain a small fraction of the charge lost by the Cu atoms. It may be noted that for the Sn atoms the charge distribution in the inner atomic region (around the core) is spherical, while the increased charge in the outer atomic region is deformed. This deformation of the electron charge density is much more pronounced for the Cu atoms than the Sn atoms. The plot also shows the electron cloud between the atoms indicating metallic character of the bonds.

On the other hand in the case of Li_2CuSn , (figure 3) the Li atoms are strongly depleted of electrons while the Cu atoms show a gain in electronic charge. The nearly spherical shape of the charge distribution indicates an ionic character of the bonds.

A comparison of the figures 2 and 3 indicates the modification in the bonding character. Lithiation of $^0\text{-Cu}_6\text{Sn}_5$ clearly results in a charge transfer from Li to the Cu and Sn atoms to form the more ionic Li_2CuSn phase. In the battery, Li is inserted as an ion with the electrons supplied from the outer circuit redistributing in the structure. In this paper we have chosen to use the term Li atoms, since the calculations are based on Li atoms within the structures.

The lithiation of $^0\text{-Cu}_6\text{Sn}_5$

According to the reactions (1) and (2), the total number of Li atoms reacting with one formula unit of Cu_6Sn_5 is 22. The experimental voltage vs. composition curve (figure 4) shows a maximum x of almost 22, which is in very good agreement with the suggested mechanisms. The in situ-XRD and Mossbauer measurements have, however, shown that the reactions taking place above 0.7V (section A in figure 4) can be attributed to surface reactions and reduction of oxides present in the sample due to the synthesis method (high-energy ball-milling) [8]. These reactions are irreversibly consuming Li and are not directly involved in reactions (1) and (2). The total experimental value for these reactions is thereby slightly smaller. The plateau, at around 0.4V (in section C of figure 4), is associated with the transformation of $^0\text{-Cu}_6\text{Sn}_5$ to Li_2CuSn . It has been suggested, that during this phase transformation, half of the Sn atoms in the $^0\text{-Cu}_6\text{Sn}_5$ structure are displaced into neighbouring Sn-strings [5, 6]. The Li_2CuSn -type phase at the end of the plateau is most likely lithium deficient, as further lithiation down to 0.2V (the sloping part in the voltage curve) results in a gradual expansion of the Li_2CuSn cubic cell axis, i.e. a solid-solution behaviour within the structure. The process below 0.2V (section D in figure 4) involves lithiation of Sn to finally yield $\text{Li}_{4.4}\text{Sn}$. We have focused mainly on the process described by reaction (1) (the Cu_6Sn_5 - Li_2CuSn transformation).

From the total energy calculations the average insertion voltage (A IV) for the Cu_6Sn_5 - Li_2CuSn transformation is calculated. The details of the method of calculation of A IV are given elsewhere [15, 16]. The calculated value of the A IV is 0.378V which, is in good agreement with the experimental value of the plateau in the voltage profile (figure 4).

In the voltage profile, the region between 0.7V and 0.4V (section B in the figure 4), i.e. after the reduction of the oxides present in the sample and before the start of the plateau, there is a sloping region involving approximately two Li atoms. This region would then correspond to the first two Li atoms inserted in the $^0\text{-Cu}_6\text{Sn}_5$ structure (i.e. x=1 to x=2 in the reaction (1)). The in situ XRD measurements in this region show that the first lithium insertion does not result in any major structural rearrangements and the $^0\text{-Cu}_6\text{Sn}_5$ peaks remain unaltered. The first-principles total energy and force calculations have been performed to study the various possibilities of how these two Li atoms are inserted into the $^0\text{-Cu}_6\text{Sn}_5$ structure. In figure 5 the calculated total valence charge density of $^0\text{-Cu}_6\text{Sn}_5$ in

the (102) plane is plotted (there exist four such planes per CUC). The minimum densities are found in the regions marked by A and B in the figure (there are 8 crystallographically symmetric sites of each kind per CUC). By looking at the charge density plots in various planes in the unit cell (not presented in the paper to keep the number of figures limited) the regions A, B and C are found to have minimum electron density and hence represents voids where the Li atoms can enter.

With this information we go on to study how well these sites incorporate a Li atom. By total energy calculations it was found that the energy requirement for the insertion of a Li atom at site A in the CUC (one Li atom per CUC corresponds to $x = 0.25$ in reaction (1) and $x = 3$ in figure 4) is 41 mRy/Li atom. On the other hand the energy required for insertion of a Li atom at site B or C in the CUC is 66 mRy/Li atom and 120 mRy/Li atom respectively. This shows that it is energetically favourable for the first two Li atoms to enter at the sites A rather than the sites B or C.

On complete relaxation of the structure with eight Li atoms per CUC (making a total of 52 atoms per CUC, i.e. $x = 2.0$ in reaction (1) and $x = 4.5$ or end of section B in figure 4) at the eight crystallographically symmetric A sites, two of which are marked in figure 5, the gain in energy is 190 mRy per $\text{Li}_2\text{Cu}_6\text{Sn}_5$ formula-unit with a volume expansion of 4.6%. In this relaxation the Sn (Sn2) atom move towards the site B, occupying the position with coordinates: 0.643, 0.450, 0.200 and the Li atom move to the position earlier occupied by the Sn (Sn2) atom. This picture supports the earlier suggestions [5, 6] about the structural rearrangement on lithiation of $^{63}\text{Cu}_6\text{Sn}_5$. However, with just two Li atoms per formula-unit there is no major structural rearrangement and the Sn atoms do not reach the sites B to form the Sn chains, but move towards sites B and come to rest nearly halfway between B and its original position (Sn2). This rearrangement is not detected experimentally.

There are two scenarios for further lithiation, one where lithium is inserted without any copper extrusion and the other where the lithium insertion is accompanied by extrusion of the CuA atoms (figure 5) from the structure. There exists no information about the morphology and the phase adopted by the extruded copper atoms, so the second case can not be studied theoretically. It was found that the first case (lithium insertion without copper extrusion i.e. 3 Li atoms per Cu_6Sn_5 formula-unit) is accompanied by a volume expansion of 47.3% and costs large amount of energy (290 mRy/Li atom) which in turn would imply a sloping voltage profile in the beginning of the section C i.e. between $x = 4.5$ to $x = 5.5$ in the figure 4 (which corresponds to $x = 2$ to $x = 3$ in reaction (1)). However, experimental voltage profile instead shows a plateau after insertion of 2 Li atoms per Cu_6Sn_5 formula-unit. We, therefore, suggest that after the insertion of two Li atoms per Cu_6Sn_5 formula unit, the Cu (CuA) atoms start to extrude from the structure accompanied by structural rearrangements.

In situ XRD measurements were performed to closely follow the phase transformation from $^{63}\text{Cu}_6\text{Sn}_5$ to Li_2CuSn . The results can be seen in figure 6, showing diffraction patterns taken at consecutive steps at the 0.4V plateau (i.e. beyond 2 Li atoms per formula-unit). On lithiation, the Cu_6Sn_5 peak at 43° gradually decrease in intensity, while the Li_2CuSn peak at 40.5° starts to increase in intensity. The data shows that the plateau corresponds to the two-phase transformation between Cu_6Sn_5 and Li_2CuSn , where half of the Sn atoms move to the neighbouring Sn chains. This transformation is accompanied by quite large structural rearrangements. The Cu_6Sn_5 peak decreases in intensity and broadens before the first sign of the Li_2CuSn phase. The diffraction peak of the resulting Li_2CuSn phase is even broader due to a more disordered phase. This supports the theoretical picture presented above.

The Mossbauer and XRD [8, 17] experiments, performed for phase determination during lithiation of $^{63}\text{Cu}_6\text{Sn}_5$, are not sensitive to the point of copper extrusion and the phase adopted by the extruded copper atoms. Since the cycling stability depends upon the copper extrusion and stability of the structure we suggest EXAFS (Extended X-ray Absorption Fine-structure Spectroscopy) and HRTEM (High-Resolution Transmission Electron Microscopy) be performed to provide more information on the exact starting point of the copper extrusion as well as the structure and morphology of the extruded copper. Further, the knowledge of the phase of the extruded copper atoms would facilitate future theoretical work on the copper deficient lithiated $^{63}\text{Cu}_6\text{Sn}_5$.

CONCLUSIONS

$^{63}\text{Cu}_6\text{Sn}_5$ is a candidate anode material for lithium-ion batteries. At a discharge voltage above 0.2V lithium-ions are inserted in $^{63}\text{Cu}_6\text{Sn}_5$ reversibly to form Li_2CuSn . In this region the cycling capacity is stable around 200 mAh/g.

From the first principles total energy and force calculations the atomic positions in $^{63}\text{Cu}_6\text{Sn}_5$ are optimised and EFG (the structure and electronic charge dependent parameter) is determined. The AIV of the $^{63}\text{Cu}_6\text{Sn}_5$ to Li_2CuSn transformation has been calculated to be 0.378V which is in good agreement with the experimental result of 0.4V.

By calculating and plotting the difference between the valence- and atomic charge in a crystal plane, the change in the bonding nature on lithiation of $^{63}\text{Cu}_6\text{Sn}_5$ could be studied. It was found that the ionicity of the bonds increases on going from $^{63}\text{Cu}_6\text{Sn}_5$ (where the bonds have metallic character) to Li_2CuSn .

Total energy and force calculations show that it is energetically favourable for the first two incoming Li atoms (two Li atoms per $^0\text{-Cu}_6\text{Sn}_5$ formula-unit) to enter at the crystallographically symmetric sites with the positional coordinate 0.907, 0.625, 0.0408. Complete relaxation of the structure leads to small structural rearrangement with the relaxation of the Sn (Sn2) atoms to occupy sites with the positional coordinate 0.643, 0.450, 0.200 and Li atoms to the positions earlier occupied by the Sn (Sn2) atoms. This leads to a large gain in energy of 190 mRy/formula-unit of $\text{Li}_2\text{Cu}_6\text{Sn}_5$ with a small volume expansion of 4.6%. Further addition of Li atoms (after two Li atoms per Cu_6Sn_5 formula-unit) without any copper extrusion from the structure costs a large amount of energy leading to a sloping voltage profile. However, the experimental voltage profile shows a plateau after $x=4.5$ (which corresponds to $x=2.0$ in reaction (1)), which suggests that after the insertion of two Li atoms per Cu_6Sn_5 formula-unit (eight Li atoms per CUC) the copper atoms are extruded from the structure leading to large structural rearrangement. This picture is supported by our XRD measurements which does not show any detectable structural change up to 2 Li atoms per Cu_6Sn_5 formula-unit but indicates a major structural rearrangement beyond that.

ACKNOWLEDGMENTS

Support for this work from The Foundation for Environmental Strategic Research (MISTRA), The Nordic Research Programme (NERP) and The Swedish Science Council (VR) is gratefully acknowledged. We are also grateful to the Swedish National Supercomputer Center in Linköping (NSC) for the use of their computational facilities. We also thank Dr. M. M. Thackeray and Dr. R. Benedek from Argonne National Laboratory, USA, for valuable comments and suggestions.

FIGURE CAPTIONS

Fig 1. The conventional unit cell of $^0\text{-Cu}_6\text{Sn}_5$. The (102) plane is marked.

Fig 2. The difference between the crystalline valence charge and the superposed atomic charge for $^0\text{-Cu}_6\text{Sn}_5$ in the (102) plane. The difference is given in the units of charge per a_0^3 , with the negative numbers in the legend indicating an increase in electrons.

Fig 3. The difference between the crystalline valence charge and the superposed atomic charge in the (110) plane of the Li_2CuSn unit cell. The difference is given in the units of charge per a_0^3 , with the negative numbers in the legend indicating an increase in electrons.

Fig 4. The voltage profile for the first discharge of a $\text{Li/Cu}_6\text{Sn}_5$ cell, x indicates number of Li atoms inserted per Cu_6Sn_5 formula unit.

Fig 5. The total valence electron charge density per a_0^3 for $^0\text{-Cu}_6\text{Sn}_5$ in the (102) plane. The six regions of low charge density are marked as A, B and C.

Fig 6. The in situ XRD data of a $\text{Li/Cu}_6\text{Sn}_5$ cell measured at the 0.4V plateau during galvanostatic discharge. The Ni peak shown is from the current collector.

-
- [1] J-M. Tarascon and M. Armand. *Nature*, 414:359, 2001.
 - [2] C. S. Johnson, J. T. Vaughey, M. M. Thackeray, T. Sarakonsri, S. A. Hackney, L. Fransson, K. Edstrom, and J. O. Thomas. *Electrochem. Comm.*, 2:595, 2000.
 - [3] J. T. Vaughey, J. O. Hara, and M. M. Thackeray. *Electrochem. Solid State Lett.*, 3:13, 2000.
 - [4] L. M. L. Fransson, J. T. Vaughey, R. Benedek, K. Edstrom, J. O. Thomas, and M. M. Thackeray. *Electrochem. Comm.*, 3:317, 2001.
 - [5] M. M. Thackeray, J. T. Vaughey, A. J. Kahaian, K. D. Kepler, and R. Benedek. *Electrochem. Comm.*, 1:111, 1999.
 - [6] K. D. Kepler, J. T. Vaughey, and M. M. Thackeray. *Electrochem. Solid State Lett.*, 2:307, 1999.
 - [7] D. Larcher, L. Y. Beaulieu, D. D. MacNeil, and J. R. Dahn. *J. Electrochem. Soc.*, 147:1658, 2000.
 - [8] L. Fransson, E. Nordstrom, K. Edstrom, L. Hagstrom and M. M. Thackeray accepted for publication in *J. Electrochem. Soc.* 2002.

- [9] P. Blaha, K. Schwarz and J. Luitz, WIEN 97, Vienna university of technology (improved and updated UNIX version of the original copyrighted wien code), published by P. Blaha, K. Schwarz, P. Sorantin, and S.B. Trickey, Comput. Phys. Commun. 59 (1990) 399.
- [10] A.K. Larsson, L. Stenberg, and S. Lidin. Acta. Cryst. B, 50:636, 1994.
- [11] H. Pauly, A. Weiss, and H. Witten. Z. Metallkde., 59:47, 1968.
- [12] R.W. G. Wyckoff, 2nd ed. Crystal Structures, Vol.1, Krieger, FL, (1982).
- [13] P. Blaha, K. Schwarz, and P. Herzig. Phys. Rev. Lett., 54:1192, 1985.
- [14] P. Blaha, P. Sorantin, C. Ambrosch, and K. Schwarz. Hyp. Int., 51:917, 1989.
- [15] G. Ceder, M.K. Aydinol, and A.F. Kohan. Comput. Mater. Sci., 8:161, 1997.
- [16] L. Benco, J.L. Barras, M. Atanasov, C. Daul, and E. Deiss. J. Solid State Chem., 145:503, 1999.
- [17] E. Nordstrom, S. Sharma, E. Sjöstedt, L. Fransson, L. Haggstrom, L. Nordstrom and K. Edstrom accepted for publication in Hyperfine Interact. 2002.

This figure "fig1.gif" is available in "gif" format from:

<http://arxiv.org/ps/cond-mat/0303091v1>

This figure "fig2.gif" is available in "gif" format from:

<http://arxiv.org/ps/cond-mat/0303091v1>

This figure "fig3.gif" is available in "gif" format from:

<http://arxiv.org/ps/cond-mat/0303091v1>

This figure "fig4.gif" is available in "gif" format from:

<http://arxiv.org/ps/cond-mat/0303091v1>

This figure "fig5.gif" is available in "gif" format from:

<http://arxiv.org/ps/cond-mat/0303091v1>

This figure "fig6.gif" is available in "gif" format from:

<http://arxiv.org/ps/cond-mat/0303091v1>